DOI: 10.13009/EUCASS2017-460

Adaptive augmentation of the attitude control system for a multirotor UAV

A. Russo[⋆], *D. Invernizzi*[⋆], *M. Giurato*[⋆] *and M. Lovera*[⋆†]
[⋆]*Dipartimento di Scienze e Tecnologie Aerospaziali, Politecnico di Milano*
Via La Masa 34, 26900 Milano, Italy

[†]Corresponding author

Abstract

In this paper the adaptive augmentation of the attitude control system for a multirotor Unmanned Aerial Vehicle (UAV) is considered. The proposed approach allows to seamlessly combine a linear robust controller with an adaptive one and to disable or enable the adaptive controller when needed, in order to take the advantages of both the controllers. Furthermore, the proposed architecture allows not only to make use of a robust controller, but any generic baseline controller that guarantees stability of the closed-loop system in nominal conditions.

1. Introduction

The problem of attitude control law design for multirotor UAVs has been studied extensively in the literature. When dealing with nominal operation, fixed-gain linear or nonlinear controllers typically suffice to solve the problem in a satisfactory way. If more challenging questions such as, *e.g.*, actuator degradation, external disturbances, parameter uncertainties, time delays and actuator faults, are to be considered, then more advanced approaches are needed. Adaptive control is an attractive candidate to face the mentioned disturbances and uncertainties because of its ability to provide high performance tracking in presence of uncertainties. Its capability of learning whilst operating, and coping with uncertainties, made adaptive control the popular choice for fault-tolerant or reconfigurable unmanned flight. In this paper, the adaptive augmentation of the attitude control system for a multirotor UAV platform is considered. The proposed approach allows to seamlessly combine a linear robust controller with an adaptive one and to disable or enable the adaptive controller when needed, in order to take the advantages of both the controllers. Furthermore, the proposed architecture allows not only to make use of a robust controller, but any generic baseline controller that guarantees stability of the closed-loop system in nominal conditions. The proposed modification is presented both for the direct Model Reference Adaptive Control (MRAC) scheme and for the indirect L_1 adaptive control scheme; in both cases, it can be applied to an existing nominal controller without any knowledge of its structure. This is a major advantage with respect to existing adaptive control schemes, which assume a fixed-structure controller, usually with proportional and integral action. The proposed adaptive scheme exploits an observer instead of a reference model, placed where the uncertainty lies. With respect to an indirect approach, the identifier is used as an observer, and it is therefore different from the usual formulation that includes the nominal dynamics of the closed-loop system.

The adaptive augmentation approach has been validated both through simulations and experiments, by comparing it to the baseline controller in nominal conditions and in case of external events. In particular, a loss of thrust was induced so to compare the behaviour of the two control schemes. Simulations were carried out using both the direct MRAC and the L_1 adaptive control. The metric to evaluate tracking performance is the amount of time it takes for the controller to reach the set point after the anomaly. Instead, the time delay margin was used to evaluate the robustness of the closed-loop system. When a MRAC scheme is employed, the numerical results confirm an improvement in the tracking performance at the cost of a reduced robustness. On the other hand, the L_1 adaptive schemes provide a better trade-off between tracking and robustness. In general, all the adaptive schemes in simulation are faster when reacting to an induced disturbance compared to the nominal controller alone. Finally, experiments were carried out, operating the quadrotor on a test-bed which constrains all translational and rotational degrees of freedom except for pitch rotation. During the tests, the angular velocity and the pitch angle, measured by the on-board IMU, were logged along with the control variable. Tests were primarily run for the L_1 adaptive control system. The results show an increase of the tracking performance when adaptive control is included.

The paper is organised as follows: first an overview of the current state of the art is given, covering mainly MRAC and $\mathcal{L}_1$ adaptive control schemes with reference to multirotor UAV systems. Subsequently the problem of adaptive augmentation is formally stated and a solution based on $\mathcal{L}_1$ adaptive control theory is presented. Finally, the results of simulations and experiment carried out to measure the improvements of the proposed adaptive control system in presence of uncertainties are presented and discussed.

2. State of the art

In the following sections some methods described in the literature to adaptively control multirotor UAVs are presented. Main results and techniques are shown for standard MRAC and $\mathcal{L}_1$ schemes.

2.1 MRAC Schemes

MRAC is the most widely known adaptive control technique and there are many interesting results in the control of multirotor UAVs. A common characteristic of MRAC schemes is the use of a baseline controller, usually a PI controller designed by means of LQR. In[7] the controller of a small quadrotor is augmented to include both a baseline fixed gain control and a model reference adaptive control. The whole system is equivalent to the baseline control in the nominal case, but in the case of a failure the adaptive control plays the role to maintain stability and regain the original performance. Although it is difficult to regain the original performance with a significant loss of thrust due to permanent damage in one of the four propellers, the Author has demonstrated that adaptive control allows for safe hover and return. Next a comparison with a CMRAC scheme was shown: the CMRAC controller was demonstrated to deliver smoother parameter estimates, allowing higher adaptive gains. It was shown that CMRAC was more effective than MRAC in learning the true value of uncertain parameters in the system, offering numerous benefits in terms of tracking performance. An equivalent scheme[8] has been proposed, which makes use of a standard baseline fixed gain control (which is a proportional plus integral controller) together with a Direct MRAC scheme. The Authors show how the adaptive controller is able to compensate uncertainties and provide better tracking performance than LQR in presence of mass uncertainty. Also in[6] a baseline fixed gain control and direct MRAC are used to demonstrate the superior performance of MRAC compared to a non-adaptive scheme in case of actuator uncertainties, with a 45% loss of thrust fault. The adaptive controller exhibits significantly less deviation from level flight. The approach was validated using flight testing inside an indoor test facility, and the Projection Operator and the Dead Zone modifications as robust tool modifications.

Of more interest are the adaptive schemes that make use of neural networks: the common denominator of those design is that the neural network is added to approximate in a single term the uncertainty of the system, such as in the $\mathcal{L}_1$ piecewise-constant adaptive control where all uncertainties are lumped into one parameter. Such approach is suitable for augmenting a baseline controller because it does not require any modification of that baseline controller and the adaptive part can be added straightforwardly. Such approach is presented for example in.[3,4,12,13] In,[34] the neural network augments a nominal PID controller. The peculiarity of those schemes is the use of the concurrent learning modification, enabling a faster converge of the estimates to their true values. The control law was designed so that an approximate inversion model is used in combination with a neural network that adaptively reduces the inversion error. Thanks to the concurrent learning modification the parameters of the neural networks converge more rapidly to their true values, leading to an improvement of the performance. In[3] this technique is tested on two quadrotors of different sizes: the baseline controller is tuned for the bigger quadrotor and then tested on the other one, which is half the size in comparison. Thanks to adaptive control nominal performance is restored, although the nominal controller was not optimised for the smaller quadrotor. The same idea is also used in[12] although without using the concurrent modification.

Instead in[13] the Authors make use of a backstepping controller that exploits adaptive techniques to control a quadrotor helicopter, successively augmented with a neural network that accounts for uncertainties. Another design that makes use of adaptive backstepping is presented in,[11] where only the mass of the vehicle is uncertain. In this work, however, the Authors do not make use of a neural network but instead model the UAV with model parameters uncertainties, leading to a more complex design of the adaptive controller since the backstepping design needs to be changed. For this reason neural networks are more beneficial, since when using them the nominal control does not have to be changed. The method in,[11] is further developed in,[5] where also the vehicle mass, inertia matrix, and aerodynamic damping coefficients are assumed to be uncertain.

A different approach for approximating the uncertainty is given in.[16] This approach makes use of a fixed gain baseline controller augmented with the CMAC: a linear function approximation used to approximate the uncertainty. In practice a CMAC is a linear combination of N functions $f_i, i = 1, \cdots, N$, where each f_i is equal to 1 inside of k square regions of input space, randomly scattered, and 0 everywhere else. Although the method shows good performance in the

DOI: 10.13009/EUCASS2017-460

presence of uncertainties, it is worth to point out that in comparison to neural networks, linear function approximation, such as CMAC, show worse performance since in general results indicate that nonlinear function approximators are more powerful for learning high-dimensional functions.

Finally, a Linear Parameter-Varying (LPV)[1] has been proposed, in which the controller, synthesised by using the structured H_∞ algorithm, is based on the fact that the controller parameters can vary in a certain domain given a set of uncertainties. Then, based on an indirect approach, by using a recursive least squares algorithm, the plant parameters are identified and used in the LPV controller. The method shows satisfactory performance and low jitter on the estimates, although no disturbances were introduced in the system.

2.2 $\mathcal{L}_1$ Adaptive Control Schemes

As for $\mathcal{L}_1$ adaptive control, there are some examples regarding UAVs, although most of them make use of a baseline control law of the type $u_b = -kx$. A different approach is shown in,[14] where a nominal backstepping controller is designed to control the attitude of the quadrotor. The baseline backstepping controller is successively augmented with a $\mathcal{L}_1$ piecewise-constant adaptive controller. Performance is visibly improved with adaptation, since fast adaptation is now possible due to the low-pass filter introduced in the $\mathcal{L}_1$ methodology. Further, also a scheme that makes use of quaternions is presented that avoids all singularities associated to Euler angles.

In[15] the Authors propose an $\mathcal{L}_1$ adaptive output feedback control design, tuned by minimizing a cost function based on the characteristics of the reference model and the low-pass filter $C(s)$. Flight test results show that the augmented $\mathcal{L}_1$ adaptive system exhibits definite performance and robustness improvements. Furthermore, the adaptive augmentation is shown to improve performance in aggressive flight.

$\mathcal{L}_1$ adaptive control has been used to control a Miniature Air Vehicle (MAV).[2] One of the main challenges for these aerial vehicles is the manufacturing process, which is not reliable enough to ensure uniform aerodynamic properties. Hence adaptive control was used to account for those uncertainties and the effectiveness of the system was demonstrated through simulation results. The $\mathcal{L}_1$ adaptive algorithm results in performance that exceeds the baseline PID controllers and exhibits robustness to a variable sample rate for the processor, as well as the time delays introduced by state estimation. The algorithm also appears to be robust with respect to state estimation errors.

Small UAVs which make use of $\mathcal{L}_1$ adaptive control[18] have also been used to collect samples of pollen, and other biological particles, up to fifty meters altitude. More precisely, in the cited work the $\mathcal{L}_1$ adaptive controller makes use of a neural network to approximate the uncertainty, with guaranteed robustness and transient performance. Simulations illustrate the control designer's ability to choose large adaptation gains for fast convergence without compromising robustness and also the fact that there is no need to re-tune the adaptive gains for different reference signals.[18]

3. Problem statement

The problem under study is to design an adaptive controller that can be seamlessly implemented in an already existing control architecture, capable of controlling the angular velocity dynamics of a multirotor UAV. For that purpose consider the Euler equations of rigid body angular motion, written in the principal inertial axes

$$I_{xx}\dot{p} + (I_{zz} - I_{yy})qr = L \tag{1}$$
$$I_{yy}\dot{q} + (I_{xx} - I_{zz})pr = M \tag{2}$$
$$I_{zz}\dot{r} + (I_{yy} - I_{xx})pq = N, \tag{3}$$

where I_{xx}, I_{yy}, I_{zz} are the principal moments of inertia, $M_{ext} = \begin{bmatrix} L & M & N \end{bmatrix}^T$ represents the external moment applied on the quadrotor vehicle and $\omega = \begin{bmatrix} p & q & r \end{bmatrix}^T$ is the body angular velocity. Letting $H_0 = \mathrm{diag}(I_{zz} - I_{yy}, I_{xx} - I_{zz}, I_{yy} - I_{xx})$ and denoting with I_n the inertia matrix, the Euler equations can be written as

$$\dot{\omega} = I_n^{-1}(M_{ext} - H_0 f(\omega)), \quad f(\omega) = \begin{bmatrix} qr & pr & pq \end{bmatrix}^T. \tag{4}$$

Note that external moments acting on the quadrotor can be decomposed into three categories: damping moment, moment due to propellers, and moment due to external disturbances. For what concerns the moment due to damping, we suppose it to be proportional to the rates ω, hence let the damping moment be given by $M_{damp} = A\omega$. The moment due to the propellers is just the control action, which will be indicated by u, hence $M_{props} = u$. Finally, external disturbances are represented by $M_d = d$. Therefore we can write

$$M_{ext} = M_{damps} + M_{props} + M_d = A\omega + u + d, \tag{5}$$

DOI: 10.13009/EUCASS2017-460

and by letting $K = I_n^{-1}, H = KH_0$, equation (4) becomes:

$$\dot{\omega} = KA\omega + Ku + Kd + Hf(\omega). \tag{6}$$

When hovering, the term $f(\omega)$ is negligible, but uncertainties and disturbances are still acting on the system, which means that the matrices K, A, H are uncertain. As for the disturbance d, in the following we will assume it to be either constant or slowly varying. Let now the subscript 0 denote nominal values, and the subscript δ the uncertainty. Then matrices A and H can be rewritten in the following way using the additive uncertainty form:

$$A = A_0 + A_\delta, \quad H = K(H_0 + H_\delta). \tag{7}$$

On the other hand, regarding K, it is usually better to express the uncertainty on the input gain in multiplicative form:

$$K = K_0\Lambda_K, \quad \Lambda_K = I + K_0^{-1}K_\delta, \tag{8}$$

so that equation (4) is rewritten as

$$\dot{\omega} = K_0\Lambda_K\Big((A_0 + A_\delta)\omega + u + d\Big) + (H_0 + H_\delta)f(\omega). \tag{9}$$

At this point suppose that for the nominal system, *i.e.*, $A_\delta = 0, H_\delta = 0, \Lambda_K = I, d = 0$, we design a baseline feedback controller $u_b(t) = C_b(r, \omega)$ capable of stabilizing the dynamics of ω, so that the DC-gain from the reference input r to ω is unitary. In addition, suppose to be in hover, so that the term $f(\omega) \approx 0$ is negligible.

The idea behind adaptive augmentation is that we want the system to operate mainly in nominal conditions, *i.e.*, to have active adaptation only when necessary. To that purpose, let the control input u be given as

$$u = u_b + u_a, \tag{10}$$

where u_b is the control action provided by the baseline controller, while u_a is the contribution to the control action given by the adaptive controller, to be designed based on the knowledge of the nominal one.

4. $\mathcal{L}_1$ augmentation design of attitude control

Based on the definition (10), consider now equation (9) and add and subtract the nominal part of the system:

$$\begin{aligned}\dot{\omega} &= K_0\Lambda_K((A_0 + A_\delta)\omega + u + d) + (H_0 + H_\delta)f(\omega) \pm K_0[A_0\omega + u_b] \\ &= \underbrace{K_0[A_0\omega + u_b]}_{\text{Nominal part}} + K_0(\alpha_1\omega + \alpha_2 u_b + \Lambda_K u_a + \tilde{d} + \alpha_3 f(\omega))\end{aligned} \tag{11}$$

where

$$\alpha_1 = (\Lambda_K - I)A_0 + \Lambda_K A_\delta \tag{12}$$
$$\alpha_2 = \Lambda_K - I \tag{13}$$
$$\alpha_3 = K_0^{-1}(H_0 + H_\delta) \tag{14}$$
$$\tilde{\sigma} = \Lambda_K d. \tag{15}$$

To take into account actuator dynamics let $G(s)$ represent the nominal transfer function of the actuator model, and let $g_b = G(s)u_b, g_a = G(s)u_a$. Uncertainties can be included in the $\tilde{d}$ term.[17] Further, we can make use of the fact that the actuator can be modeled as an uncertain input gain, and thus rewrite the previous equation as

$$\dot{\omega} = K_0[A_0\omega + g_b] + K_0(\alpha_1\omega + \alpha_2 g_b + \lambda u_a(t) + \tilde{d} + \alpha_3 f(\omega)), \tag{16}$$

where λ is a parameter used in $\mathcal{L}_1$ adaptive control to model the uncertain input gain.[10] Notice that Λ_K is included in λ.

4.1 Design of the filter $C(s)$

We know[10,17] we can design the filter $C(s)$ so that the reference system is stabilized. In our case the reference system is given by

$$\dot{\omega} = K_0[A_0\omega + g_b] + K_0(\alpha_1\omega + \alpha_2 g_b + \lambda u_a(t) + \tilde{d} + \alpha_3 f(\omega)) \tag{17}$$
$$u_a(s) = -\frac{1}{\lambda}C(s)(\alpha_1\omega + \alpha_2 g_b + \tilde{d} + \alpha_3 f(\omega)) \tag{18}$$

DOI: 10.13009/EUCASS2017-460

and $C(s)$ needs to be a proper stable filter with DC-gain $C(0) = 1$. Further, the reference system should be stable for all the possible unknown dynamics of the actuator. Let F_Δ denote the set of possible dynamics of the actuator, with $G(s) \in F_\Delta$, then $C(s)$ has the following structure:

$$C(s) = \frac{KF(s)D(s)}{1 + KF(s)D(s)} \tag{19}$$

with $F(s) \in F_\Delta, K > 0$ user chosen and $D(s)$ selected as

$$D(s) = \frac{1}{s} \tag{20}$$

to satisfy the assumption of DC-gain $C(0) = 1$. In our case the actuator was modeled as a low pass filter, with constant time delay and a zero-order hold

$$G(s) = \frac{1}{\tau_n s + 1} \frac{1 - e^{st_s}}{st_s} e^{-st_s}, \tag{21}$$

whilst the nominal control is given by the output of a PID controller $R_{\mathrm{PID}}(s)$

$$u_b(s) = G(s)R_{\mathrm{PID}}(s)(\omega_r(s) - \omega(s)), \tag{22}$$

with ω_r being the reference signal. Let then

$$R(s) = G(s)R_{\mathrm{PID}}(s), \tag{23}$$

and

$$H(s) = (sI - K_n A_n + K_n R(s))^{-1} K_n, \quad M(s) = 1 - C(s) \tag{24}$$

from which it follows that

$$\omega(s) = H(s)R(s)\omega_r(s) + H(s)M(s)(\alpha_1\omega + \alpha_2 R(s)(\omega_r(s) - \omega(s)) + \tilde{d} + \alpha_3 f(\omega)). \tag{25}$$

Next, define

$$G_1(s) = H(s)R(s) + H(s)M(s)R(s)\alpha_2, \quad G_2(s) = H(s)M(s)R(s) \tag{26}$$

and

$$G_3(s) = H(s)M(s). \tag{27}$$

If $G_d(s)$

$$G_d(s) = (I + G_2(s)\alpha_2 - G_3(s)\alpha_1)^{-1}, \tag{28}$$

is a stable transfer function for all possible values of α_1, α_2, then the reference system is stable. Based on the fact that $G_1(s)$ is stable we can calculate the $\mathcal{L}_1$ norm of $G_d(s)G_1(s)$ and check for which K it goes to infinity. Recall that for $K = 0$ the system is still stable since we are considering uncertainties that do not destabilise the system.

4.2 Predictor model and control law

To build the predictor model consider the plant model given in equation (16); based on that expression the observer-predictor

$$\dot{\hat{\omega}} = K_0[A_0\hat{\omega} + g_b] + K_0(\hat{\alpha}_1\omega + \hat{\alpha}_2 g_b + \hat{\lambda}u_a(t) + \hat{\tilde{d}} + \hat{\alpha_3} f(\omega)) + Le(t) \tag{29}$$

is used, where $\hat{\alpha}_1, \hat{\alpha}_2, \hat{\lambda}, \hat{\tilde{\sigma}}, \hat{\alpha_3}$ are the estimates of $\alpha_1, \alpha_2, \lambda, \tilde{\sigma}, \alpha_3$.

Further, let L be a Hurwitz matrix, added to increase the convergence rate of the error dynamics, where the error is defined as

$$e(t) = \hat{\omega}(t) - \omega(t) \tag{30}$$

then, based on that, the error dynamics is modelled by

$$\dot{e} = (K_0 A_0 + L)e + K_0(\Delta\alpha_1\omega + \Delta\alpha_2 g_b + \Delta\lambda u_a(t) + \Delta\tilde{d} + \Delta\alpha_3 f(\omega)). \tag{31}$$

Finally, the adaptive control law is defined as

$$u_a(s) = -KD(s)\eta(s), \quad \eta(s) = \hat{\alpha}_1\omega + \hat{\alpha}_2 g_b + \hat{\lambda}u_a(t) + \hat{\tilde{d}} + \hat{\alpha_3} f(\omega), \tag{32}$$

where K and $D(s)$ are chosen as discussed in Section 4.1. On the other hand the value for L was chosen to be $L = -50I$, after several simulations.

4.3 Adaptive laws

Based on the error equation (31), the adaptive laws

$$\dot{\hat{\alpha}}_1 = \text{Proj}(\hat{\alpha}_1, -\Gamma_1 \omega(t) e(t)^T PB) \tag{33}$$
$$\dot{\hat{\alpha}}_2 = \text{Proj}(\hat{\alpha}_2, -\Gamma_2 g_b e(t)^T PB) \tag{34}$$
$$\dot{\hat{\alpha}}_3 = \text{Proj}(\hat{\alpha}_3, -\Gamma_3 f(\omega(t)) e(t)^T PB) \tag{35}$$
$$\dot{\hat{\lambda}} = \text{Proj}(\hat{\lambda}, -\Gamma_4 u_a(t) e(t)^T PB) \tag{36}$$
$$\dot{\hat{\sigma}} = \text{Proj}(\hat{d}, -\Gamma_5 e(t)^T PB), \tag{37}$$

are used. The uncertain parameter λ, which is the equivalent gain of the propellers dynamics, is given initial value 1 and for simplicity its bound is $\lambda \in [0.1, 2]$.

5. Simulation results

The considered quadrotor, see Figure 1, weights approximately 1.5 kg and has an arm length of 0.28 m. In particular, both simulations and experiments were conducted on a single axis of the quadrotor, to control the pitch attitude. As shown in Figure 1 all the translational and rotational DoFs were constrained except for pitch rotation.

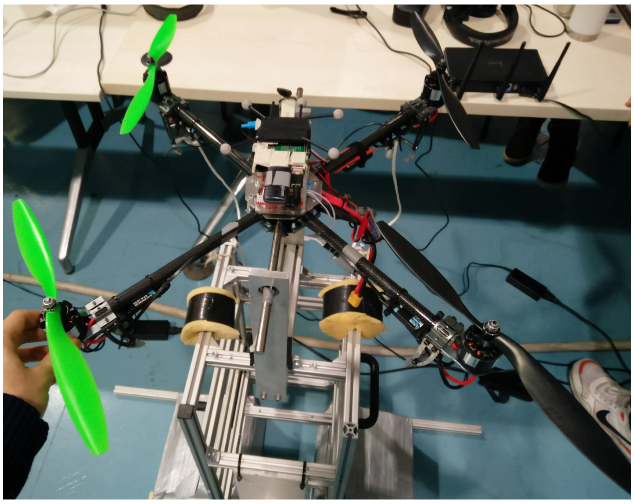

Figure 1 – Quadrotor used for the tests.

In the simulation study two different adaptive augmentation schemes have been considered, namely the $\mathcal{L}_1$ adaptive scheme outlined in Section 4 and a similar MRAC adaptive augmentation scheme.[17] Both augmentation schemes have been implemented on top of a structured robust H_∞ linear controller.[9] To assess the performance of the adaptive approaches, a pulse-wave step signal has been used as a reference input, with amplitude of 30°. At 7 seconds a load of 0.5 kg has been attached to the 3rd arm of the quadrotor, acting as a disturbance to be rejected by the control system. In Table 1 are shown some performance indicators, that are also evident from Figure 2. The reaction time is defined as the amount of time that occurs from the beginning of the disturbance (which starts at $t_0 = 7$) to the maximum error peak between the desired response and $\Theta(t)$. From results the adaptive controller is about 3.3 times faster than the nominal controller to cancel the uncertainty. Further, the maximum error peak between $\Theta(t)$ and the desired response with MRAC is about a fifth of the peak obtained with the nominal controller. Moreover, the average error, from t_0 to $t_0 + 3$ is dramatically decreased: the adaptive controller is able to keep the mean error to a value that is more than 10 times lower than the one of the nominal controller. Finally notice from Figure 2 that

$$\sup_{t\in[0,20]} e(t) \approx 0.12\,\text{rad}\,\text{s}^{-1}.$$

Regarding the load disturbance the $\mathcal{L}_1$ adaptive control design shows comparable performance to the MRAC scheme. Some performance indicators are shown in Table 2 and the most significant difference between the $\mathcal{L}_1$ and MRAC designs is a slight increase of the average error. The adaptive control is 3.1 times faster than the nominal

DOI: 10.13009/EUCASS2017-460

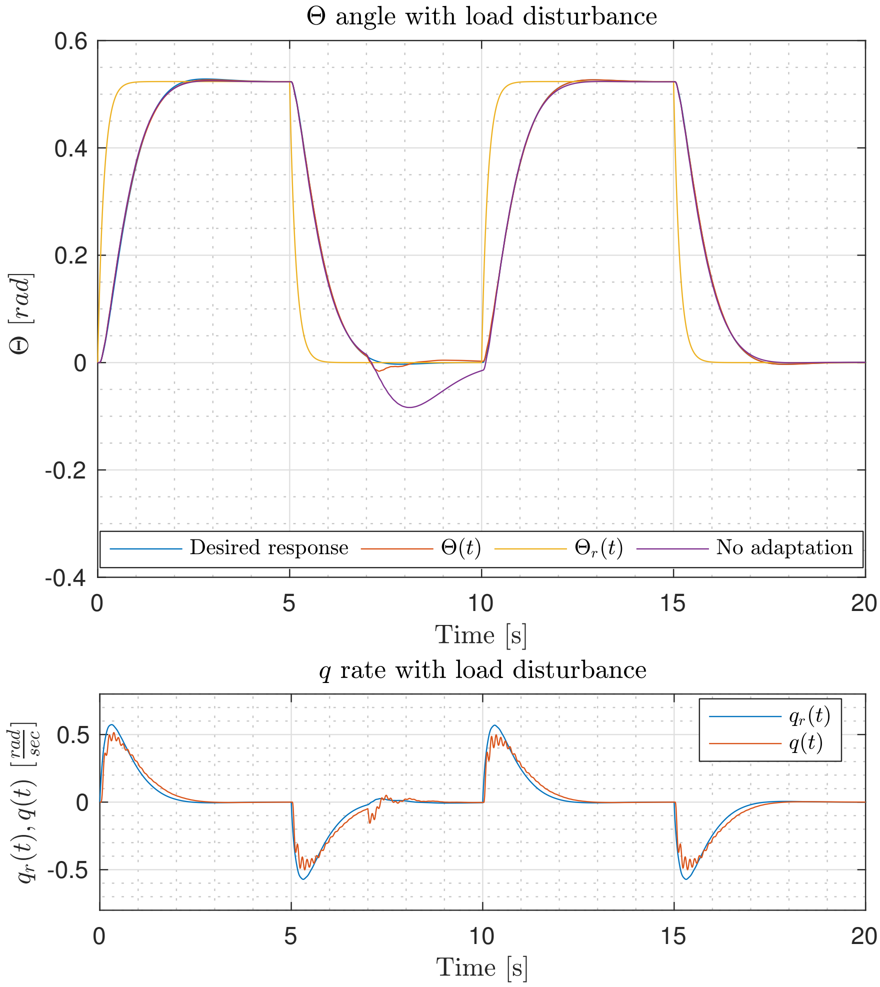

Figure 2 – Response of the system on a single axis using the MRAC scheme. At 7 seconds a load of 0.5 kg is attached to one of the arms of the quadrotor.

Load Disturbance	Reaction Time	Maximum error	Average error
Adaptive Enabled	0.32 s	0.91°	0.25°
Adaptive Disabled	1.07 s	4.61°	2.80°

Table 1 – MRAC - Load disturbance: Performance improvements

DOI: 10.13009/EUCASS2017-460

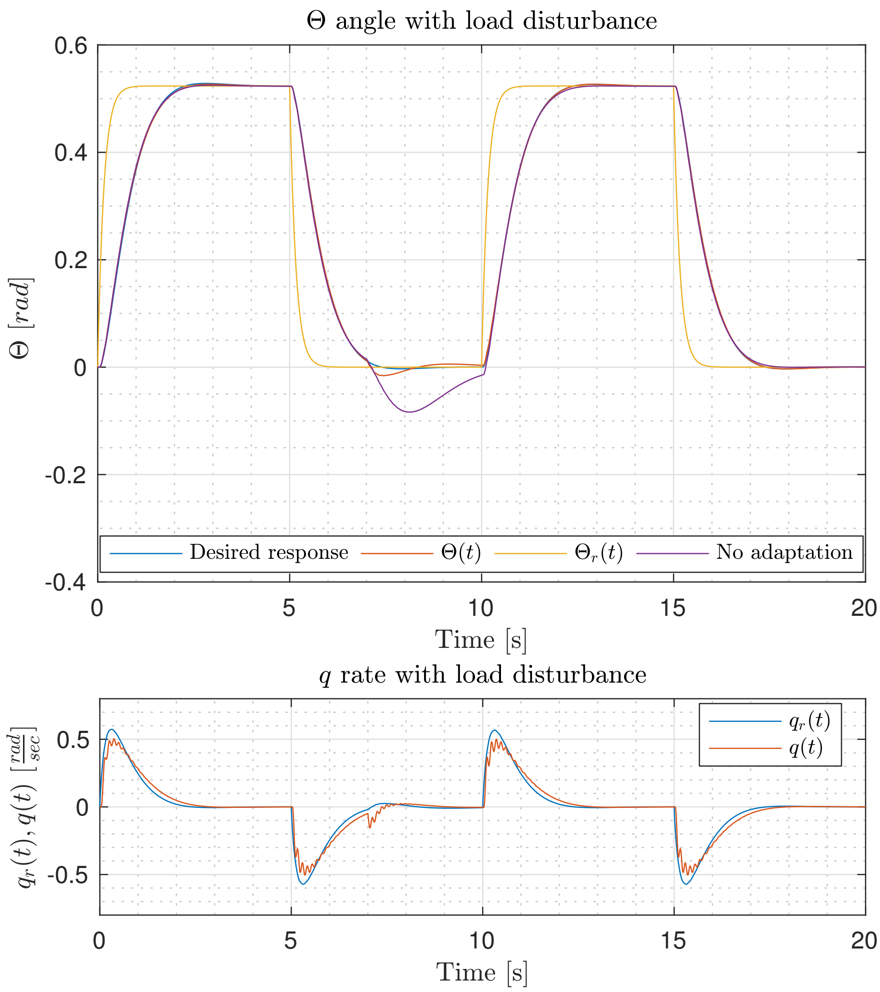

Figure 3 – Response of the system on a single axis using the $\mathcal{L}_1$ scheme. At 7 seconds a load of 0.5 kg is attached to one of the arms of the quadrotor.

DOI: 10.13009/EUCASS2017-460

controller, and the maximum error peak is again about a fifth of the peak obtained with the nominal controller. The average error, computed from t_0 to $t_0 + 3$, is still very low: the adaptive controller is able to keep the mean error to a value that is about 7.6 times lower than the one of the nominal controller. This performance is perfectly explained by the fact that we are using a low-pass filter to cut-off the higher frequencies of the estimates, in this way we are not perfectly cancelling the uncertainties during the transient. Finally notice from Figure 3 that

$$\sup_{t\in[0,20]} e(t) \approx 0.04\,\mathrm{rad\,s^{-1}},$$

lower than the one obtained with the MRAC controller, due to fact that the matrix L was changed so to quicken the error dynamics.

Load Disturbance	**Reaction Time**	**Maximum error**	**Average error**
Adaptive Enabled	0.35 s	0.93°	0.37°
Adaptive Disabled	1.07 s	4.61°	2.80°

Table 2 – $\mathcal{L}_1$ - Load disturbance: Performance improvements

The time delay margin is comparable to the MRAC design, although there are some improvements as shown in Table 3. Compared to the nominal controller we have the same time delay margin for the nominal case, whilst when ϕ_m is minimised the delay margin drops of about one-third. It should be noted that for different values of K different values of the time delay margin are obtained. In fact K is the tuning knob that adjusts the trade-off between performance and robustness.

Time Delay Margin	**Nominal case**	**Min ϕ_m case**
τ_m	$0.03s$	$0.02s$

Table 3 – $\mathcal{L}_1$ Time Delay Margin

6. Experimental results

The $\mathcal{L}_1$ adaptive control scheme was chosen to be tested on the real quadrotor.[9] The quadrotor was tested mainly for two types of disturbances: a loss of throttle in the motors, which implies a loss of thrust, and the robustness of the adaptive control to non-linear effects, such as not being in hovering condition.

The quadrotor software architecture was designed with the possibility to *virtually* remove a percentage of throttle from one or more propellers. More precisely, knowing that[9] the throttle of a motor is related to its rotational speed by

$$\Omega = mT_{h\%} + q \tag{38}$$

where $T_{h\%}$ is the throttle percentage, and $q, m \in \mathbb{R}$ are static calibration parameters,[9] the on-board software of the quadrotor actually implements

$$\Omega = m(T_{h\%} + d) + q, \tag{39}$$

where $d \in [-100, 100]$ is a command, external to the control loop, given to increase or decrease the throttle. Therefore it is a percentage value and acts as a loss or gain of thrust. Notice that in hover we have that $\Omega = \Omega_0 \approx 387.84\,\mathrm{rad\,s^{-1}}$, therefore the throttle value is

$$T_{h\%_0} = \frac{\Omega_0 - q}{m} = 50.96\%. \tag{40}$$

Given that thrust is proportional to the square of rotational speed

$$T \propto \Omega_0^2, \tag{41}$$

due to d we have a multiplicative uncertainty γ on the rotational speed

$$T \propto (\gamma\Omega_0)^2, \tag{42}$$

DOI: 10.13009/EUCASS2017-460

which implies a loss of thrust for $\gamma < 1$. It is straightforward to notice that

$$\gamma = \frac{\Omega}{\Omega_0} = \sqrt{1 + \frac{m^2 d^2 + 2m^2 T d + 2mqd}{\Omega_0^2}}, \tag{43}$$

where a plot of γ^2 is given in Figure 4.

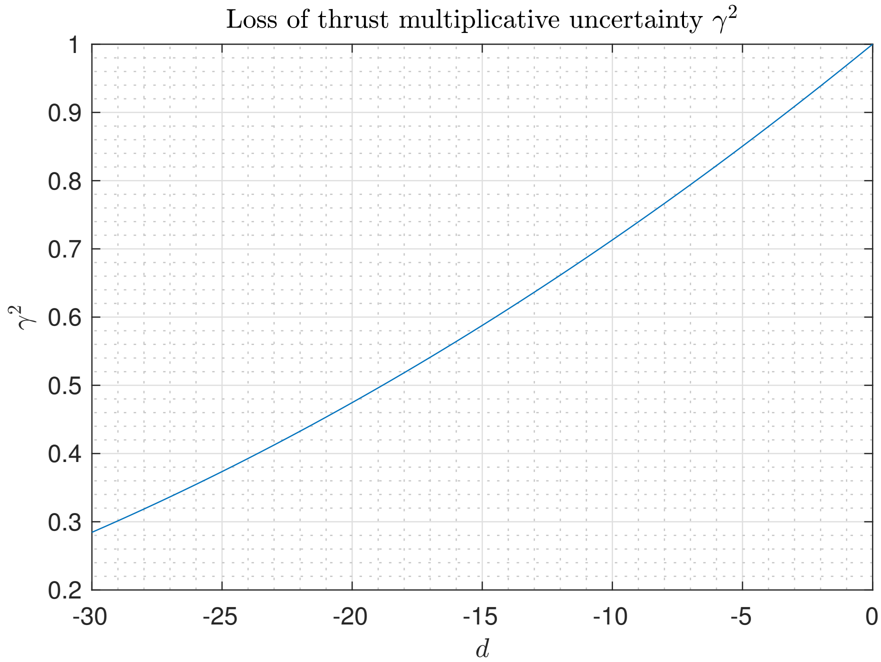

Figure 4 – Loss of thrust γ^2 due to the disturbance d in hover. For example for $d = -12\%$ there is about 34% loss of thrust in hover.

Based on that, two experiments were designed:

- *Steady state control*: during the experiment the set point of the pitch angle Θ is set to 0. After about 10 seconds to the second motor a disturbance $d = -12\%$ is applied, which implies a loss of thrust of 34%. Then, approximately after 20 seconds the disturbance is removed. The test is done in order to verify the ability of the adaptive control to quickly recover the attitude.
- *Pulse-wave step reference control*: in this test a pulse-wave step reference input is used to control the pitch angle Θ with amplitude of $28°$ (0.5 rad). At the mid of the test a disturbance $d = -12\%$ is applied to the second motor. The test is done so to verify both the ability of the adaptive control to quickly recover the attitude and to suppress the influence of nonlinearities on the pitch angle.

As previously stated, results for the augmented $\mathcal{L}_1$ adaptive control will be presented. Due to unmodeled dynamics and delays it was found necessary to lower the value K of the $\mathcal{L}_1$ low-pass filter to values below 2. Other than that, the other parameters of the controller were chosen as:

$$K = 0.7, \quad L = -125, \quad \varepsilon = 0.9, \quad \Gamma = 10^5, \tag{44}$$

where ε is an attribute of the Projection Operator, defining when the projection should start. The bounds used for the estimates are:

$$\hat{\alpha}_1 \in [-0.2, 0.2] \tag{45}$$
$$\hat{\alpha}_2 \in [-0.2, 0.2] \tag{46}$$
$$\hat{\lambda} \in [0.8, 1.2] \tag{47}$$
$$\hat{\sigma} \in [-0.4, 0.4]. \tag{48}$$

In Figure 5 the plot of the pitch angle signal is shown, whilst Figure 6 illustrates the time history of the control signal M. First notice the quickness of the adaptive control to counteract the disturbance. It should be noted, though,

DOI: 10.13009/EUCASS2017-460

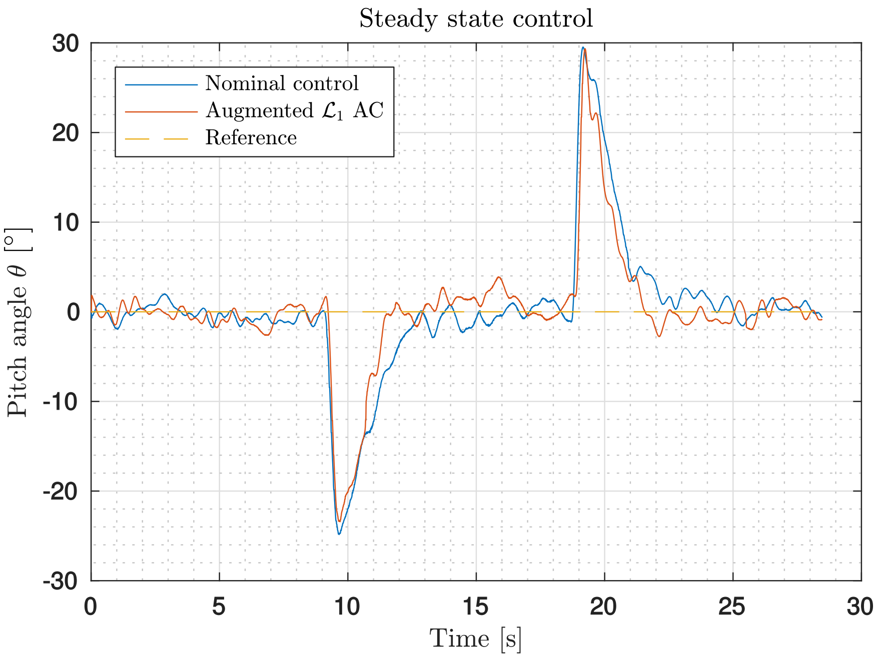

Figure 5 – Plot of the pitch angle Θ. At about 9 seconds a disturbance $d = -12\%$ is applied. Notice the quick response of the $\mathcal{L}_1$ adaptive control.

that the estimates are being low-pass filtered at a very low frequency since $K = 0.7$. Despite that there is a visible improvement of the tracking performance. The variance ratio of the two signals was used as indicator: let Θ_a be the pitch angle signal obtained using adaptive control, whilst Θ_n the one using the nominal control. Then we obtain that the Mean Squared Error (MSE) is

$$\mathbb{E}[\Theta_a^2] \approx \frac{1}{N}\sum_{i=1}^{N}\Theta_{i,a} \approx 40, \quad \mathbb{E}[\Theta_n^2] \approx \frac{1}{N}\sum_{i=1}^{N}\Theta_{i,n} \approx 50.2 \tag{49}$$

where Θ_i is the i-th sample, and N the total number of samples. Then:

$$\frac{\mathbb{E}[\Theta_a^2]}{\mathbb{E}[\Theta_b^2]} \approx 0.72, \tag{50}$$

which indicates that effectively we have better tracking performance, despite the modelled dynamics and the not-optimized parameters. In Figure 6 it is possible to notice that overall the adaptive control law does not heavily modify the baseline control signal, acting only at high frequencies. Let M_a and M_n be the control signal respectively of the adaptive control and the nominal control. We have that

$$||M_a||_2 = \sqrt{\int_0^T |M_a(t)|^2 dt} \approx 3.42, \quad ||M_n||_2 = \sqrt{\int_0^T |M_n(t)|^2 dt} \approx 3.49, \tag{51}$$

which indicates that the energy used by the two control schemes is almost the same. Further, it should be noted that during the disturbance period of time the dc-frequency amplitude is higher for M_n than M_a.

In the second experiment, the results of which are shown in Figure 7, the set-point used for the pitch angle is more similar to what was used during the simulations. A pulse-wave step reference input signal was used, with amplitude of about 28°, which breaks the hovering assumption. At about 24 seconds a disturbance $d = -12\%$ is applied to the second propeller. Although from figure it is not clearly visible the adaptive control action improves the reaction time of the nominal controller of about 25%. Unfortunately, the nominal control used in this test is similar to the one used in the simulations, but it is not exactly the same. Further, the value of K was lowered, which means that the adaptive controller is more robust at the cost of performance. All of this implies that necessarily performance will not be the same of the simulations presented in the previous chapter. Despite that, notice that when the set point is about 28° the nominal controller is not able to follow the reference properly, due to nonlinearities. That effect on the other hand is suppressed by the adaptive control, which is able to track the reference signal. Now, let Θ_a denote the pitch angle

DOI: 10.13009/EUCASS2017-460

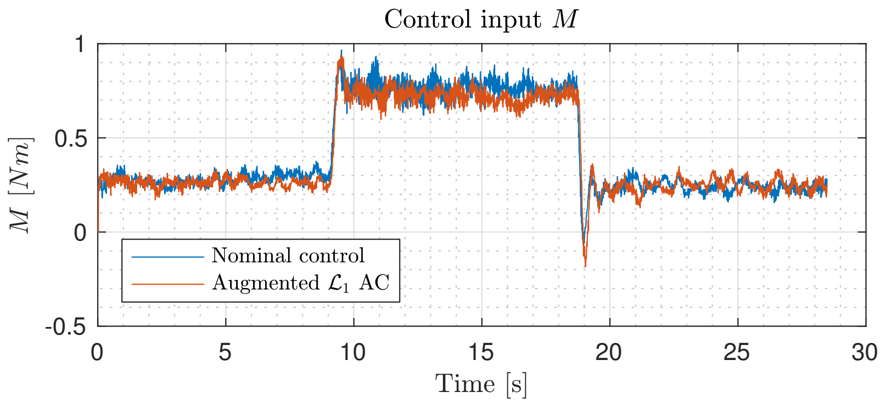

Figure 6 – Control signal M. Notice the similar behaviour of the two different types of control for low frequencies.

signal when adaptive control is used, Θ_n the pitch angle when nominal control is used and Θ_0 the reference signal. The MSEs are:

$$\mathbb{E}[(\Theta_a - \Theta_0)^2] \approx \frac{1}{N}\sum_{i=1}^{N}(\Theta_{i,a} - \Theta_{i,0})^2 \approx 19.43$$

$$\mathbb{E}[(\Theta_a - \Theta_0)^2] \approx \frac{1}{N}\sum_{i=1}^{N}(\Theta_{i,n} - \Theta_{i,0})^2 \approx 23.77$$

which indicates a performance increase of about 20%. In Figure 8 the control signal for the two control schemes is shown, and overall the two schemes at low frequencies are the same, as expected. A further indication is that the energy of the two signals is almost the same:

$$\|M_a\|_2 = \sqrt{\int_0^T |M_a(t)|^2 dt} \approx 4.08, \quad \|M_n\|_2 = \sqrt{\int_0^T |M_n(t)|^2 dt} \approx 3.90. \tag{52}$$

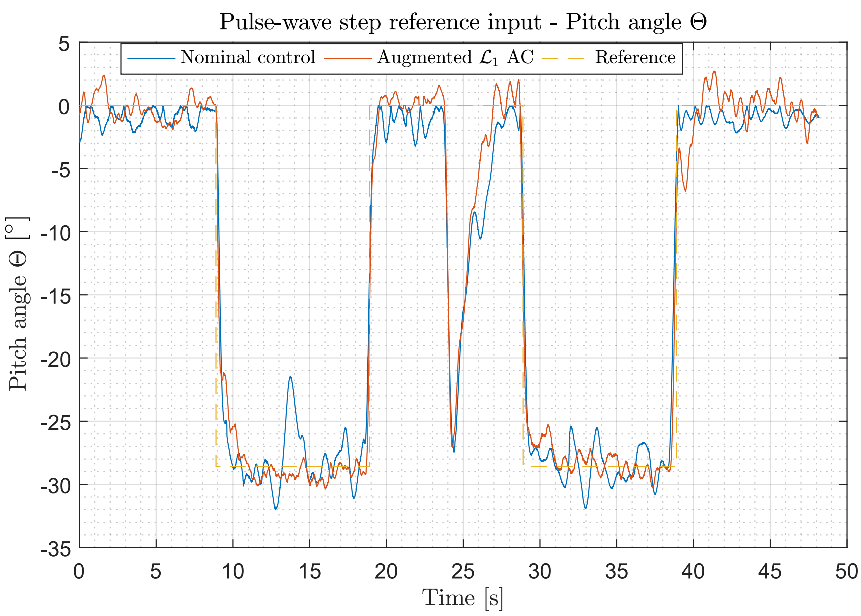

Figure 7 – Plot of the pitch angle Θ during a pulse-wave step reference input. In red the adaptive control, blue the nominal control. At about 24s a 34% loss of thrust is applied to the second motor.

DOI: 10.13009/EUCASS2017-460

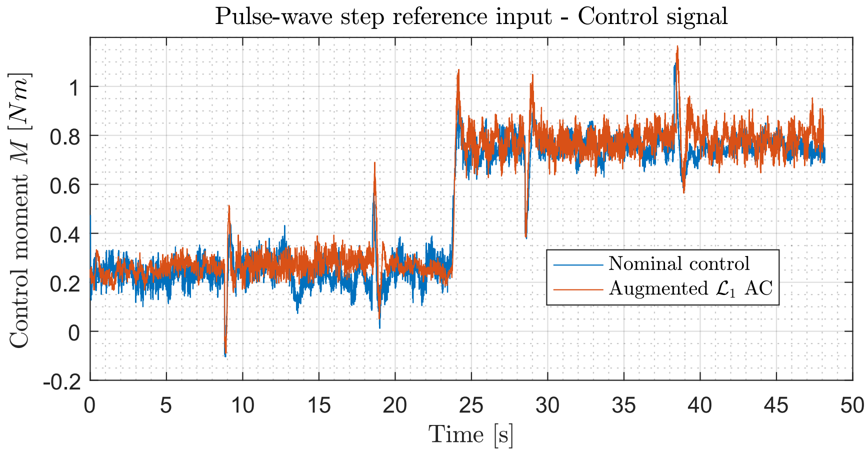

Figure 8 – Plot of the control signal moment M during a pulse-wave step reference input. In red the adaptive control, blue the nominal control. At about 24s a 34% loss of thrust is applied to the second motor.

7. Conclusions

In conclusion, the proposed implementation requires only a little increase in terms of control power, although few modifications of the control scheme are needed. Overall, the adaptive controllers developed in this work offer an increased robustness to parametric uncertainties and they are effective in mitigating a loss-of-thrust anomaly compared to the nominal controller alone.

References

[1] Y. Ameho, F. Niel, F. Defaÿ, J.-M. Biannic, and C. Bérard. Adaptive control for quadrotors. In *2013 IEEE International Conference on Robotics and Automation (ICRA)*, pages 5396–5401. IEEE, 2013.

[2] R. W. Beard, N. B. Knoebel, C. Cao, N. Hovakimyan, and J. S. Matthews. An l_1 adaptive pitch controller for miniature air vehicles. In *AIAA Guidance, Navigation, and Control Conference, Keystone, CO*, 2006.

[3] G. Chowdhary, T. Wu, M. Cutler, N. K. Ure, and J. How. Experimental results of concurrent learning adaptive controllers. In *AIAA Guidance, Navigation, and Control Conference (GNC),(Minneapolis, MN), AIAA*, 2012.

[4] G. V. Chowdhary and E. N. Johnson. Theory and flight-test validation of a concurrent-learning adaptive controller. *Journal of Guidance, Control, and Dynamics*, 34(2):592–607, 2011.

[5] C. Diao, B. Xian, Q. Yin, W. Zeng, H. Li, and Y. Yang. A nonlinear adaptive control approach for quadrotor UAVs. In *2011 8th Asian Control Conference (ASCC)*, pages 223–228. IEEE, 2011.

[6] Z. T. Dydek, A. M. Annaswamy, and E. Lavretsky. Adaptive control of quadrotor UAVs in the presence of actuator uncertainties. *AIAA Infotech@ Aerospace*, pages 20–22, 2010.

[7] Z. T. Dydek, A. M. Annaswamy, and E. Lavretsky. Adaptive control of quadrotor UAVs: A design trade study with flight evaluations. *IEEE Transactions on Control Systems Technology*, 21(4):1400–1406, 2013.

[8] A. A. Ghaffar and T. Richardson. Model reference adaptive control and LQR control for quadrotor with parametric uncertainties. *World Academy of Science, Engineering and Technology, International Journal of Mechanical, Aerospace, Industrial, Mechatronic and Manufacturing Engineering*, 9(2):244–250, 2015.

[9] M. Giurato. Design, integration and control of a multirotor UAV platform. Master's thesis, Politecnico di Milano, Italy, 2015.

[10] N. Hovakimyan and C. Cao. *L_1 adaptive control theory: guaranteed robustness with fast adaptation*, volume 21. Siam, 2010.

[11] M. Huang, B. Xian, C. Diao, K. Yang, and Y. Feng. Adaptive tracking control of underactuated quadrotor unmanned aerial vehicles via backstepping. In *American Control Conference*, pages 2076–2081, 2010.

DOI: 10.13009/EUCASS2017-460

[12] E. N. Johnson and S. K. Kannan. Adaptive trajectory control for autonomous helicopters. *Journal of Guidance, Control, and Dynamics*, 28(3):524–538, 2005.

[13] T. Madani and A. Benallegue. Adaptive control via backstepping technique and neural networks of a quadrotor helicopter. In *17th IFAC World Congress, Seoul, South Korea*, 2008.

[14] S. Mallikarjunan, B. Nesbitt, E. Kharisov, E. Xargay, N. Hovakimyan, C. Cao, et al. L_1 adaptive controller for attitude control of multirotors. In *AIAA Guidance, Navigation and Control Conference, Minneapolis, AIAA-2012-48312012*, 2012.

[15] B. Michini and J. How. L_1 adaptive control for indoor autonomous vehicles: design process and flight testing. In *Proceeding of AIAA Guidance, Navigation, and Control Conference*, pages 5754–5768, 2009.

[16] C. Nicol, C. Macnab, and A. Ramirez-Serrano. Robust adaptive control of a quadrotor helicopter. *Mechatronics*, 21(6):927–938, 2011.

[17] A. Russo. Adaptive control of multirotor UAVs. Master's thesis, Politecnico di Milano, Italy, 2017.

[18] J. Wang, V. Patel, C. A. Woolsey, N. Hovakimyan, and D. Schmale. L_1 adaptive control of a UAV for aerobiological sampling. In *2007 American Control Conference*, pages 4660–4665. IEEE, 2007.